

Push-Pull-Allenenes: The Influences of Substituents on the Activation of Allenes by Biomimetic Zinc Complexes

Burkhard O. Jahn^{a,b}, Wilhelm A. Eger^{a,c}, and Ernst Anders^a

^a Institute of Organic Chemistry and Macromolecular Chemistry, Friedrich Schiller University Jena, Humboldtstraße 10, 07743 Jena, Germany

^b Institute of Organic Chemistry and Biochemistry AS CR, v.v.i Flemingovo namesti 2, 16610 Prague, Czech Republic

^c School of Chemistry and Molecular Bioscience, University of Queensland, St. Lucia, Brisbane, QLD 4072, Australia

Reprint requests to Prof. Dr. Ernst Anders. Fax: +49 3641 948212. E-mail: ernst.anders@uni-jena.de

Z. Naturforsch. **2010**, *65b*, 425–432; received November 11, 2009

Dedicated to Professor Rolf W. Saalfrank on the occasion of his 70th birthday

The influence of substituents at the allene skeleton on the rate-determining step of the reaction with nucleophiles catalyzed by biomimetic zinc complexes was investigated with quantum chemical (especially DFT) methods. Additional examinations were applied to derivatives of the zinc hydroxide complex modeled in analogy to the catalytic center of carbonic anhydrase. Especially suitable substituents in the allene moiety can lead to a significant lowering of the activation barrier. Further we demonstrate that by the application of this principle of a bioanalogous enhancement of reactivity other nucleophiles instead of the biological substrate can also be reactants in completely closed catalytic reaction cycles.

Key words: Allenes, Substitution Effects, Carbonic Anhydrase, Cumulene Activation

Introduction

In a recent paper we investigated and discussed in detail the biomimetic hydration reaction of allene catalyzed by zinc complexes modeled in analogy to the active center of the enzyme carbonic anhydrase (CA) [1]. The resulting reaction cascades were derived from the biological paradigm, *i. e.* the addition of water to the heterocumulenic system carbon dioxide under the influence of special zinc complexes as catalysts which are synthetically accessible. The enzyme CA is able to accelerate this fundamental biological reaction by a factor of up to 10^7 [2, 3]. Not only this property illustrates the enormous potential for a biomimetic translation of natural model reactions which may result in efficient synthetic procedures.

The results for the unsubstituted allene show a remarkably expressed catalytic effect for the initial attack on the terminal carbon atoms as well as at the central carbon atom. The difference in activation energy $\Delta\Delta G$ between the competing transition states is about 20 kJ mol^{-1} . The initial attack on allene represents the rate-determining step in each variant of the

reaction pathways. In this publication we describe effects of substitution on the energetically lower lying transition state of the nucleophilic attack on the central carbon atom of allene. The zinc complex-catalyzed reaction of allene with nucleophiles stands in the context of the biomimetic activation of a wide variety of isoelectronic cumulenes by carbonic anhydrase (CA) models [4–10].

Allene with its isomer methyl acetylene accrues in large amounts in the C3-cut of the naphtha distillation [11]. Currently both compounds are only hydrogenated to propene and propane, respectively, or flared off [12]. Therefore the biomimetic activation of allene has a strong economical aspect.

Especially Saalfrank *et al.* shaped at the beginning of the 1970's the concept of "push-pull" allenenes for allenenes with electron releasing and withdrawing substituents on different ends of the molecule [13–16] and therefore initiated some aspects of the investigations presented here.

As a matter of principle, examinations of substitution effects on the reaction of allene with nucleophiles are not limited to allene itself, but can be ex-

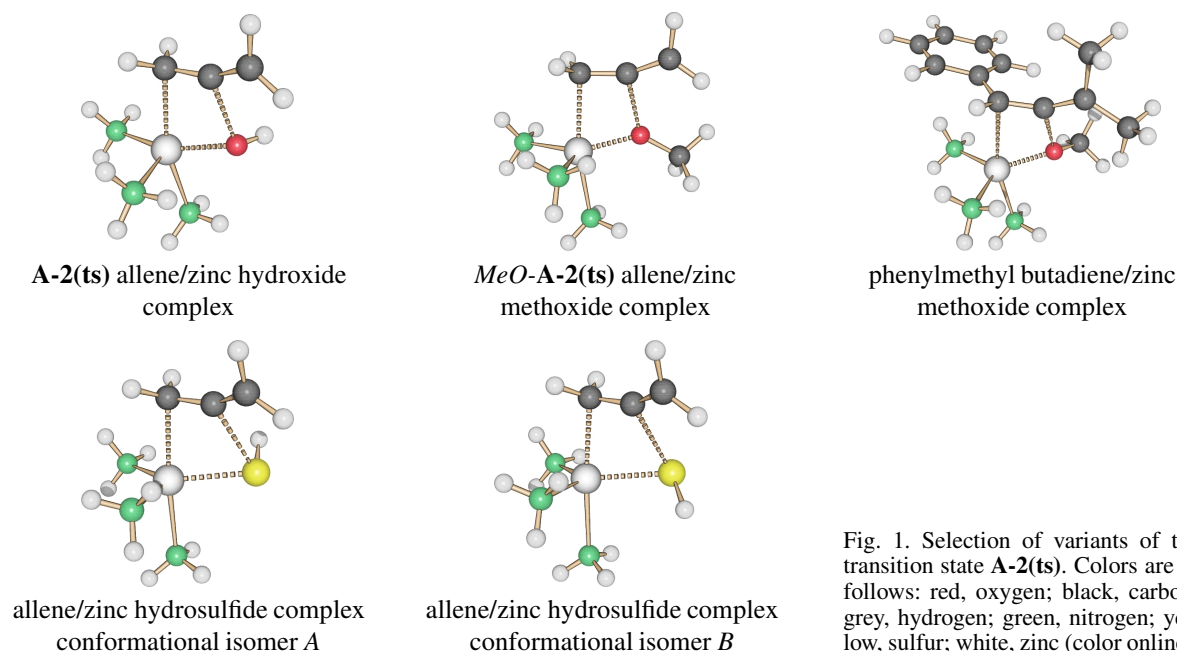


Fig. 1. Selection of variants of the transition state **A-2(ts)**. Colors are as follows: red, oxygen; black, carbon; grey, hydrogen; green, nitrogen; yellow, sulfur; white, zinc (color online).

tended to modifications of the nucleophilic ligand of the zinc model complex. For example, Teles *et al.* found an activation of allene on silica gel with zinc acetate in methanol and obtained 2-methoxypropene and 2,2-dimethoxypropene in 85 % yield [17].

Results and Discussion

Computational details

All geometry optimizations of intermediates and transition states were carried out using the mPW1k functional (modified Perdew-Wang 1-parameter for kinetics) [18] in combination with the augmented CC-pVDZ basis set [19–21]. The hybrid density mPW1k functional is especially capable to give reliable results for kinetics and energy barriers. It is based on the Perdew-Wang exchange functional [22] with Adamo and Barone's modified enhancement factor [23] and the Perdew-Wang correlation functional [22]. A larger percentage of Hartree-Fock exchange has been introduced to circumvent the underestimated barrier heights typical of standard exchange-correlation functionals. All calculations were performed using the GAUSSIAN 03 [24] program package. Additionally, NBO analyses were performed using NBO 5.0 [25]. Stable structure geometries were characterized by a frequency analysis.

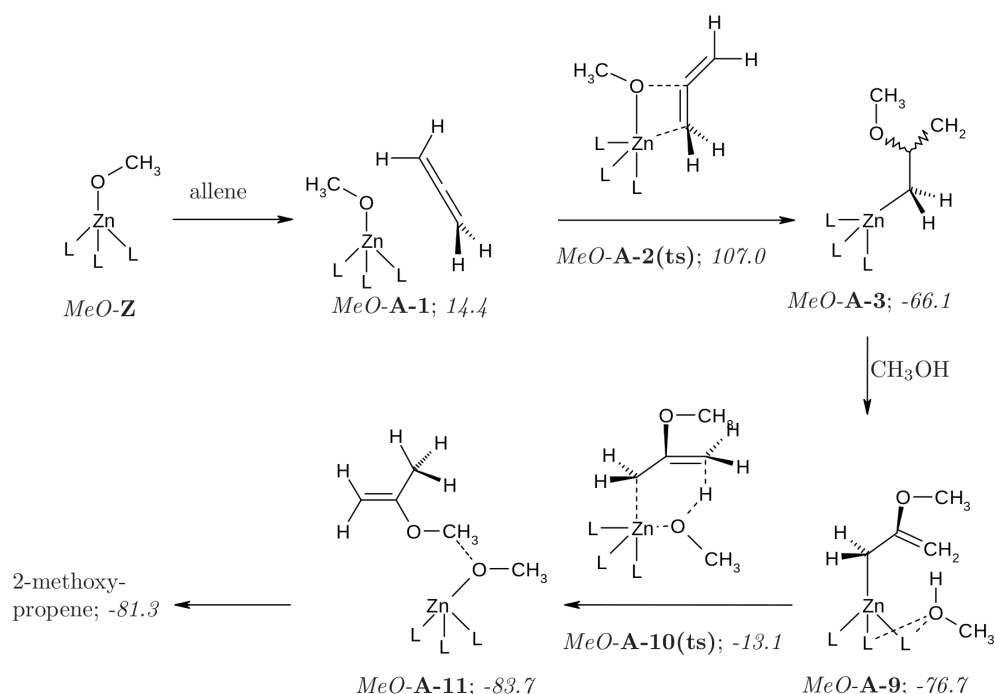
Equation $E^{(2)} = -n_{lp} \frac{F_{ij}^2}{\Delta\epsilon}$ describes the $E^{(2)}$ estimation used in this publication for characterization of orbital interactions, n_{lp} is the occupancy number of the lone pair, F_{ij} the Fock matrix element between orbitals i and j , and $\Delta\epsilon$ is the energy gap between the two interacting orbitals.

The ammonia model was used as a theoretical model for the elaborate CA enzyme. The zinc atom is complexed by the nucleophilic ligand as well as three ammonia molecules in place of the histidine amino acids.

For comparability reasons, the nomenclature used here is identical to that applied in ref. [1].

Substituted allenenes – influences on the transition state **A-2(ts)**

For the investigation of influences on the initial transition state **A-2(ts)** of the reaction between allene and the zinc model complex (see Fig. 1, *c.f.* also Scheme 1 which contains most of the important reaction steps for the example of the methoxide catalyst instead of the zinc hydroxide complex, *e.g.* the **MeO-A-2(ts)**) we used the methyl group as an example for a residue with a positive inductive and no mesomeric effect. Allene modifications arising from a positive mesomeric effect in connection with negative induction will be presented exemplarily by the substitutions with bromine and a



Scheme 1. Complete catalytic cycle of the zinc methoxide complex-catalyzed reaction of methanol with allene. Structure *MeO-A-3* is chiral (the two waved line bonds stand for an up and a down wedge; *c.f.* [1]). ΔG in kJ mol^{-1} , $L = \text{NH}_3$.

phenyl residue, respectively. The results of our calculations for transition state **A-2(ts)** of differently substituted allenenes are collected in Table 1.

The symmetrical substitution of allene on both terminal carbon atoms with bromine leads to a negligible change in the natural charge of the central carbon. However, the electron-withdrawing effect of the electronegative halogen atoms causes a less negative partial charge on the terminal carbons. Although the absolute value of the differences in natural charge of the outer and inner carbons between allene and 1,3-dibromoallene remains nearly the same in the transition states, distinct differences in the geometries can be observed, particularly for the Zn-C and C-O bonds. 1,3-Dibromoallene as the educt notably shortens the C-O distance ($\Delta d = 0.121 \text{ \AA}$, see Table 1). On the other hand the distance between the zinc ion and the terminal carbon atom is extended by more than about 0.3 \AA to $d = 2.578 \text{ \AA}$ compared to the unsubstituted allene. These different bond lengths result from a stronger attraction between one lone pair of the oxygen atom (NBO $lp_3(\text{O})$, HOMO of the zinc model complex) and the π^* orbital of the attacked double bond (LUMO of the allene molecule). Another factor influencing the activation barrier of the transition state is the weaken-

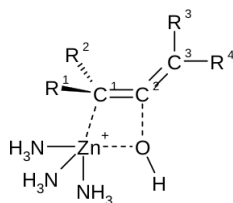
ing of the interaction between the $\pi(\text{CC})$ bond orbital (HOMO of the allene molecule) and a nearly unoccupied orbital of the zinc ion with antibonding character (denoted by NBO analysis as $lp^*(\text{Zn})$). In the transition states between allene and the zinc model complexes, NBO $lp^*(\text{Zn})$ represents the residual orbital at the Zn atom resulting from the fission of the Zn-O bond. For $lp^*(\text{Zn})$ the orbital coefficient of the oxygen atom amounts only to about 2%, and the total occupation is 0.3 e. On that score, the NBO analysis describes this orbital as a lone pair at the zinc ion.

Nevertheless, the symmetric substitution of allene with bromine leads not to a significant difference in the activation energies ($\Delta\Delta G = 0.9 \text{ kJ mol}^{-1}$), as those influences compensate each other.

On the other hand, mono-substitution with bromine causes a small lowering of the activation energy due to the higher dipole moment of the molecule ($\Delta\Delta G = 7.1 \text{ kJ mol}^{-1}$). Due to a slightly stronger interaction energy between the $\pi(\text{CC})$ and the $lp^*(\text{Zn})$ orbitals, the Zn-C distance is somewhat shorter compared to the dibromoallene case ($d = 2.539 \text{ \AA}$). The bonding situation regarding the distance between the central carbon and the oxygen atom is reversed compared to the case with a symmetric substitution. However, the allenic carbon

Table 1. Substitution effects of allenenes concerning the transition state **A-2(ts)**.

Educt	Allene	Dibromoallene (R ¹ , R ³ = Br)	Bromoallene (R ¹ = Br)	Hydroxide Complex		
				Bromobutadiene (R ¹ = Br; R ³ = CH ₃)	Bromobutadiene (R ¹ = CH ₃ ; R ³ = Br)	Phenylbutadiene (R ¹ = Ph; R ³ = CH ₃)
ΔG^\ddagger ^a	123.9	123.0	116.8	111.7	147.4	105.2
d_{C^2O} ^b	2.071	1.950	1.975	2.000	1.963	1.934
d_{ZnO} ^b	1.941	1.916	1.911	1.917	1.949	1.919
$d_{C^1C^2}$ ^b	1.363	1.344	1.349	1.350	1.360	1.370
Δd_{CC} ^b	0.060	0.046	0.051	0.053	0.056	0.060
d_{ZnC^1} ^b	2.271	2.578	2.539	2.458	2.319	2.478
$\angle OZnC^1$ ^b	79.7	71.9	72.5	75.0	78.6	74.0
$\angle OC^2C^1$ ^b	103.5	108.2	105.9	105.7	107.3	107.5
$\times ZnOC^2C^1$ ^b	17.6	19.8	28.4	22.8	26.8	16.2
$\delta_{NC}(Zn)$ ^c	1.63	1.63	1.64	1.64	1.63	1.64
$\delta_{NC}(O)$ ^c	-1.21	-1.14	-1.16	-1.17	-1.15	-1.14
$\delta_{NC}(C^2)$ ^c	0.23	0.11	0.15	0.14	0.17	0.20
$\delta_{NC}(C^1)$ ^c	-0.91	-0.68	-0.71	-0.72	-0.66	-0.64
$\Delta E^{(2)}lp_3(O)/\pi^*(C^1C^2)$ ^d	223.4	311.2	278.3	281.4	278.5	327.9
$\Delta E^{(2)}lp_2(O)/\pi^*(C^1C^2)$ ^d	51.2	47.5	40.7	40.8	48.9	45.1
$\Delta E^{(2)}\pi(C^1C^2)/lp^*(Zn)$ ^d	206.4	87.0	92.4	116.6	212.8	163.2



^a ΔG^\ddagger in kJ mol^{-1} ; ^b bond lengths in Å, angles in deg; ^c natural charge; ^d $\Delta E^{(2)}$ in kJ mol^{-1} .

framework is notably twisted out of the ZnOC plane (ZnOCC dihedral angle $a = 28.4^\circ$).

The introduction of a methyl group leads to a further lowering of the activation barrier by about 5 kJ mol^{-1} (Table 1). Alkyl residues normally have a positive inductive effect on aromatic systems. Due to its aromaticity, a phenyl group possesses a negative inductive effect. Nevertheless in the same manner the electron-releasing potential of the electron-rich allenyl group dominates over that of the methyl group.

Accordingly, the natural charge of the methyl-substituted allenic carbon atom of 1-bromobuta-1,2-diene amounts to $\delta_{NC} = -0.23$ (Table 3). Therefore the regioselective attack of the zinc cation at the bromine-substituted carbon is favored compared to the methyl-substituted carbon by about 30 kJ mol^{-1} , although there are strong orbital interactions (Table 1).

The calculations show that a further lowering of the activation barrier could be achieved by substituting bromine with a phenyl group. The difference in activation energy between 1-bromobuta-1,2-diene and 1-phenylbuta-1,2-diene amounts to $\Delta\Delta G = 6.5 \text{ kJ mol}^{-1}$. The highest energy of orbital interaction between $lp_3(O)$ and the π^* orbitals of the attacked double bond

of all six calculated transition states with the zinc hydroxide complex is $\Delta E^{(2)} = 327.9 \text{ kJ mol}^{-1}$ in the case of 1-phenylbuta-1,2-diene.

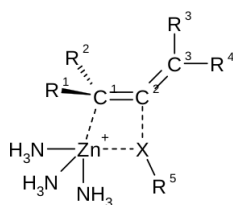
Alternative nucleophilic ligands at the zinc catalyst – influences on the transition state **A-2(ts)**

Alternatively to substitutions on the allene moiety, the nucleophilic ligand of the zinc complex can be varied. Calculations were performed with zinc complexes bearing a methoxide, hydrosulfide, and methylthiolate moiety instead of the hydroxide ligand (Table 2).

Substitution of hydroxide by a methoxide leads to a significant lowering of the activation barrier of the transition state **A-2(ts)**. This TS is energetically located only $\Delta G^\ddagger = 107.0 \text{ kJ mol}^{-1}$ higher than the separated educts, and therefore $\Delta\Delta G = 16.9 \text{ kJ mol}^{-1}$ is more favorable in comparison to the hydroxide complex. Differences in the charge distribution can only be discovered at the zinc-bound oxygen. The negative partial charge of this oxygen decreases by 20%. Equally the energy of the donor-acceptor interaction between the $\pi(CC)/lp^*(Zn)$ orbitals and the $lp_3(O)/\pi^*(CC)$ orbitals of the Zn-C and O-C distances decreases.

Table 2. Substitution effects of the nucleophilic ligand concerning the transition state **A-2(ts)**.

Educt	Methoxide Complex (X = O; R ⁵ = CH ₃)			Hydrosulfide Complex (X = S; R ⁵ = H)		Methylthiolate Complex (X = S; R ⁵ = CH ₃)	
	Allene	Dibromoallene (R ¹ = Br; R ³ = Br)	Phenylmethylbutadiene (R ¹ = Ph; R ³ , R ⁴ = CH ₃)	Allene	Allene	Allene	Allene
Conformation				A	B	A	B
ΔG^\ddagger ^a	107.0	112.1	104.2	155.4	158.5	148.6	146.7
d_{C^2X} ^b	2.037	1.941	1.961	2.397	2.381	2.416	2.336
d_{ZnX} ^b	1.906	1.897	1.905	2.346	2.346	2.310	2.293
$d_{C^1C^2}$ ^b	1.358	1.340	1.367	1.376	1.379	1.370	1.367
d_{ZnC^1} ^b	2.308	2.678	2.483	2.264	2.263	2.330	2.391
$\angle XZnC^1$ ^b	76.4	68.9	73.0	83.4	82.0	83.7	76.5
$\angle XC^2C^1$ ^b	99.3	107.2	104.2	105.5	103.6	106.4	99.7
$\times ZnXC^2C^1$ ^b	20.2	27.3	19.6	30.7	33.0	32.6	44.9
$\delta_{NC}(Zn)$ ^c	1.64	1.65	1.64	1.55	1.55	1.54	1.54
$\delta_{NC}(X)$ ^c	-0.98	-0.95	-0.96	-0.64	-0.62	-0.40	-0.38
$\delta_{NC}(C^2)$ ^c	0.24	0.12	0.21	0.10	0.11	0.07	0.08
$\delta_{NC}(C^1)$ ^c	-0.91	-0.64	-0.61	-0.95	-0.97	-0.92	-0.90
$\Delta E^{(2)}lp_3(X)/\pi^*(C^1C^2)$ ^d	187.6	272.2	256.2	566.1	521.4	494.6	426.6
$\Delta E^{(2)}\pi(C^1C^2)/lp^*(Zn)$ ^d	151.3	59.3	141.8	207.2	208.8	146.2	95.8



^a ΔG^\ddagger in kJ mol⁻¹; ^b bond lengths in Å, angles in deg; ^c natural charge; ^d $\Delta E^{(2)}$ in kJ mol⁻¹.

In contrast, the interaction between the second lone pair of the oxygen atom and the π^* orbital of the attacked CC bond becomes stronger. Due to these facts, a marginal elongation of the Zn-C and a shortening of the O-C bond can be observed. As the changes of the remaining geometrical parameters are negligible, the lowering of the activation energy is exclusively an electronic effect of the methoxide ligand.

Replacement of the allene by 1,3-dibromoallene leads to a small increase of the resulting activation barrier. The decrease in electron density at the terminal carbon atom elongates the Zn-C distance by about 0.4 Å. Even the ZnOCC dihedral angle is notably enlarged in comparison to the geometry of the transition state with unsubstituted allene. Nevertheless, the ligand exchange of hydroxide by methoxide causes also a lowering in activation energy for 1,3-dibromoallene.

The calculation of the transition state for 1-phenyl-3-methylbuta-1,2-diene and the methoxide complex gives the lowest activation barrier of all presented transition states of substituted allenes with CA-analogous model complexes ($\Delta G^\ddagger = 102.2$ kJ mol⁻¹, see Table 2). In comparison to 1-phenylbuta-1,2-diene, introduction

Table 3. Natural charges δ_{NC} for allene and selected substituted allenes. The total charge of the molecules is composed of the localized charges of the discrete atoms. Therefore differences from charge neutrality are caused by the properties of the remaining substituents (not shown).

	C ¹	C ²	C ³
Allene	-0.51	0.07	-0.51
1,3-Dibromoallene	-0.35	-0.01	-0.35
1-Bromoallene	-0.40	0.03	-0.45
1-Bromobuta-1,2-diene	-0.38	0.01	-0.23
1-Phenylbuta-1,2-diene	-0.30	0.07	-0.28
1-Phenyl-3-methyl buta-1,2-diene	-0.29	0.07	-0.10

of a second methyl group leads to a further decrease of the partial charge at the terminal carbon atom ($\delta_{NC} = -0.1$), but the Zn-C distance ($d = 2.483$ Å) remains as long as observed in the transition state of the hydroxide complex with bromoallene or phenylbutadiene. Contrary to dibromoallene, the $\pi(CC)/lp^*(Zn)$ interaction is more than twice as strong.

Exchanging oxygen by sulfur in the nucleophilic ligand has a significant influence on the reaction parameters. As both ligands, the hydrosulfide and methylthiolate ion, possess a lower partial charge at the sulfur atom, which is a result of its lower electronegativity, the energy barriers of the corresponding tran-

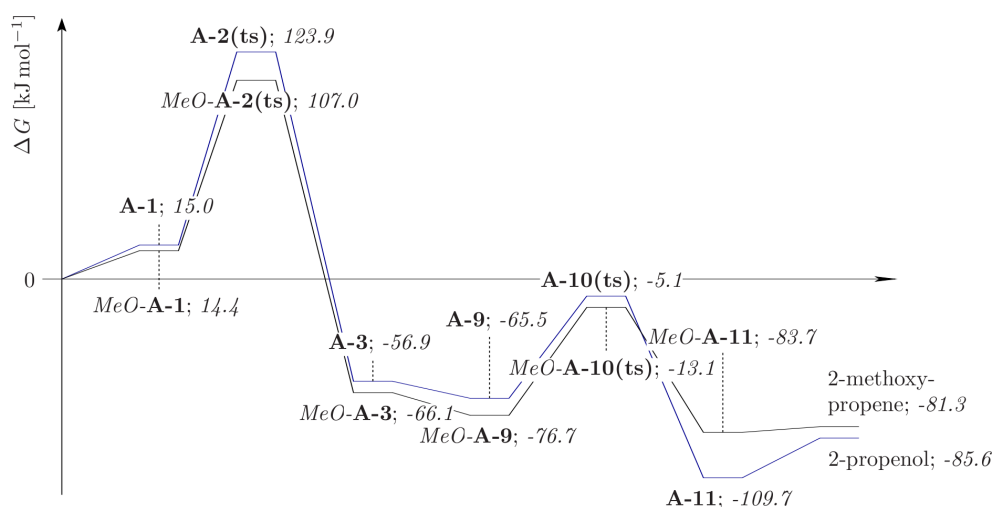


Fig. 2. Energetic profile of the zinc methoxide complex-catalyzed reaction of methanol with allene in comparison to the zinc hydroxide complex for the ammonia model ($L = \text{NH}_3$).

sition states are about $\Delta\Delta G = 30\text{--}40\text{ kJ mol}^{-1}$ higher than for the examples with the hydroxide and methoxide ions. Hence in the case of the methyl thiolate ion the partial charge differs by $\delta_{\text{NC}} = -0.6$ and -0.4 , respectively, when examining the complex bearing a hydrosulfide ligand. Additionally, the bond lengths increase by about 0.4 \AA compared to oxygen donors. Obviously, there is a strong interaction between the HOMO of the allene molecule, π^* (CC), and a lone pair which is located at the sulfur atom and results from the breaking of the Zn-S bond. In case of the methylthiolate complex this association energy $\Delta E^{(2)}$ amounts to over 500 kJ mol^{-1} . This interaction represents the linkage of the generating C-S bond. Similar to the situation with the hydroxide and methoxide complex, the activation energies of the transition states also decrease from the hydrosulfide to the methylthiolate complex. Additionally, the interaction between the π (CC) orbital and the almost empty (*vide supra*) lp^* (Zn) of the zinc ion is weaker and thus resulting in a longer Zn-C bond in the transition state.

For both the hydrosulfide and the methylthiolate complexes two transition states have been located, which both differ only by the position of the hydrogen atom and the methyl group, respectively, as they are bonded perpendicularly to the S-C allene contact. Hence the transition states *A* and *B* differ only in the orientation of this angle (Fig. 1). Apparently, this is a result of the *p* character of the lone pair at the sulfur atom (92.9% *p* character according to the NBO analysis).

The catalytic cycle of the zinc methoxide complex with allene

As shown before, the replacement of the hydroxide ligand by a methoxide ion causes a significant decrease in activation energy of the transition state **A-2(ts)**. To compare these two model complexes, we calculated the whole pathway starting from **A-9** via **A-10(ts)** to **A-11** for both compounds (Scheme 1) [1]. To develop conditions which should allow a complete catalytic cycle, we chose methanol as a proton source for the last step in which the catalyst should be regenerated.

In the geometry of the encounter complex (EC) *MeO-A-1* the position of the allene relative to the ligand sphere resembles the situation with the hydroxide complex. In comparison to the hydroxidic structure **A-1**, it is slightly more stable, and the central carbon atom forms a slightly shorter bond to the oxygen atom (Scheme 1 and Fig. 2).

Starting from EC *MeO-A-1*, intermediate *MeO-A-3* can be generated via the transition state *MeO-A-2(ts)*. As mentioned previously, the activation barrier of this TS is about $\Delta\Delta G = 16.9\text{ kJ mol}^{-1}$ lower in energy compared to the reaction of the hydroxide complex. The geometry of the intermediate *MeO-A-3* resembles the structure of **A-3** very well. Especially the ZnCCC dihedral angle does not differ between the structures obtained by the ammonia model or the theoretical and experimental triazacyclododecane model [26, 27]. The energies of both the intermediate and the following encounter complex *MeO-A-9* are

stabilized by about $\Delta\Delta G = 10 \text{ kJ mol}^{-1}$ compared with the analogous stage of the catalytic cycle mediated by the hydroxide complex. Also the energy of the consecutive six-membered cyclic transition state *MeO-A-10(ts)* is lowered by about the same difference ($\Delta\Delta G = 8 \text{ kJ mol}^{-1}$). All the structures do not differ very much, as most variations are comparable to those between *MeO-A-2(ts)* and *A-2(ts)*. Contrary to this trend, the encounter complex *MeO-A-11* between the product 2-methoxypropene and the model complex *MeO-Z* is $\Delta\Delta G = 26 \text{ kJ mol}^{-1}$ higher than the analogous structure *A-11*. The main reason for that is a hydrogen bond between the hydroxide ion of the zinc complex and the product 2-propenol. In case of the methoxide complex such stabilizing interactions are not possible.

Conclusions

From the new results and our previous findings, we conclude that the reaction principles of carbonic anhy-

dase are applicable to a wide variety of molecules isoelectronic with CO_2 . Further variants of nucleophilic moieties at the central zinc cation besides the hydroxide ion are possible (*e. g.* OR, SH and SR). This may result in novel synthetic procedures which add value to allene as a by-product of industrial purification processes. Further, Saalfrank's interesting "push-pull" allenens should be applied and investigated in this context for novel synthetic applications. Therefore we are sure that our DFT investigations of biomimetic reactions presented here, which are based on the carbonic anhydrase mode of action, will serve as a paragon for further research on biochemical model systems and their potential application in synthesis.

Acknowledgements

Financial support by the Deutsche Forschungsgemeinschaft and the Fonds der Chemischen Industrie (Germany) is gratefully acknowledged.

-
- [1] B. O. Jahn, W. A. Eger, E. Anders, *J. Org. Chem.* **2008**, *73*, 8265–8278.
- [2] S. Lindskog, *Pharmacology & Therapeutics* **1997**, *74*, 1–20.
- [3] J.-Y. Liang, W. N. Lipscomb, *J. Am. Chem. Soc.* **1986**, *108*, 5051–5058.
- [4] S. Sinnecker, M. Bräuer, W. Koch, E. Anders, *Inorg. Chem.* **2001**, *40*, 1006–1013.
- [5] D. Schröder, H. Schwarz, S. Schenk, E. Anders, *Angew. Chem. Int. Ed.* **2003**, *42*, 5087–5090; *Angew. Chem.* **2003**, *115*, 5241–5244.
- [6] S. Schenk, J. Kesselmeier, E. Anders, *Chem. Eur. J.* **2004**, *10*, 3091–3105.
- [7] G. Miscione, M. Stenta, D. Spinelli, E. Anders, A. Bottoni, *Theor. Chem. Acc. Theor. Comput. Model. Theor. Chim. Acta* **2007**, *118*, 193–201.
- [8] J. Notni, S. Schenk, G. Protoschill-Krebs, J. Kesselmeier, E. Anders, *ChemBioChem* **2007**, *8*, 530–536.
- [9] S. Schenk, J. Notni, U. Köhn, K. Wermann, E. Anders, *Dalton Trans.* **2006**, 4191–4206.
- [10] W. A. Eger, B. O. Jahn, E. Anders, *J. Mol. Model.* **2009**, *15*, 433–446.
- [11] T. Shimizu, S. Takahashi, Y. Sezaki, K. Yamamoto, Patent JP 60218336 (A), **1985**.
- [12] S. Hatscher, M. Hesse, Patent WO 2008009568 (A1), **2008**.
- [13] R. W. Saalfrank, H. Maid, *Chem. Commun.* **2005**, 5953–5967.
- [14] R. W. Saalfrank, *Tetrahedron Lett.* **1975**, *16*, 4405–4408.
- [15] R. W. Saalfrank, *Angew. Chem.* **1974**, *86*, 162–163. *Angew. Chem., Int. Ed. Engl.* **1974**, *13*, 143–144;
- [16] R. W. Saalfrank, *Tetrahedron Lett.* **1973**, *14*, 3985–3988.
- [17] K. Breuer, J. H. Teles, D. Demuth, H. Hibst, A. Schäfer, S. Brode, H. Domgörgen, *Angew. Chem. Int. Ed.* **1999**, *38*, 1401–1405; *Angew. Chem.* **1999**, *111*, 1497–1502.
- [18] B. Lynch, P. Fast, M. Harris, D. Truhlar, *J. Phys. Chem. A* **2000**, *104*, 4811–4815.
- [19] T. H. Dunning, Jr., *J. Chem. Phys.* **1989**, *90*, 1007–1023.
- [20] R. A. Kendall, T. H. Dunning, Jr., R. J. Harrison, *J. Chem. Phys.* **1992**, *96*, 6796–6806.
- [21] K. B. Wiberg, *J. Comput. Chem.* **2004**, *25*, 1342–1346.
- [22] J. P. Perdew, J. Chevary, S. Vosko, K. A. Jackson, M. R. Peterson, D. Singh, C. Fiolhais, *Phys. Rev. B* **1992**, *46*, 6671.
- [23] C. Adamo, V. Barone, *J. Chem. Phys.* **1998**, *108*, 664–675.
- [24] M. J. Frisch, G. W. Trucks, H. B. Schlegel, G. E. Scuseria, M. A. Robb, J. R. Cheeseman, J. A. Montgomery, Jr., T. Vreven, K. N. Kudin, J. C. Burant, J. M. Millam, S. S. Iyengar, J. Tomasi, V. Barone, B. Menonucci, M. Cossi, G. Scalmani, N. Rega, G. A. Petersson, H. Nakatsuji, M. Hada, M. Ehara, K. Toyota, R. Fukuda, J. Hasegawa, M. Ishida, T. Nakajima, Y. Honda, O. Kitao, H. Nakai, M. Klene, X. Li, J. E. Knox, H. P. Hratchian, J. B. Cross, C. Adamo, J. Jaramillo, R. Gomperts, R. E. Stratmann, O. Yazyev, A. J. Austin, R. Cammi, C. Pomelli, J. W. Ochterski,

- P. Y. Ayala, K. Morokuma, G. A. Voth, P. Salvador, J. J. Dannenberg, V. G. Zakrzewski, S. Dapprich, A. D. Daniels, M. C. Strain, O. Farkas, D. K. Malick, A. D. Rabuck, K. Raghavachari, J. B. Foresman, J. V. Ortiz, Q. Cui, A. G. Baboul, S. Clifford, J. Cioslowski, B. B. Stefanov, G. Liu, A. Liashenko, P. Piskorz, I. Komaromi, R. L. Martin, D. J. Fox, T. Keith, M. A. Al-Laham, C. Y. Peng, A. Nanayakkara, M. Challacombe, P. M. W. Gill, B. Johnson, W. Chen, M. W. Wong, C. Gonzalez, J. A. Pople, GAUSSIAN03 (revision B.04), Gaussian Inc., Wallingford, CT (USA) **2004**.
- [25] E. D. Glendening, J. K. Badenhoop, A. E. Reed, J. E. Carpenter, J. A. Bohmann, C. M. Morales, F. Weinhold, Weinhold, NBO 5.0, University of Wisconsin, Madison, WI (USA) **2001**.
- [26] J. E. Richman, T. J. Atkins, *J. Am. Chem. Soc.* **1974**, *96*, 2268 – 2270.
- [27] E. Kimura, T. Shiota, T. Koike, M. Shire, M. Kodama, *J. Am. Chem. Soc.* **1990**, *112*, 5805 – 5811.